Impact of vegetation variability on potential predictability and skill of EC-Earth simulations

Martina Weiß, Bart van den Hurk, Reindert Haarsma, Wilco Hazeleger

Royal Netherlands Meteorological Institute (KNMI), De Bilt, The Netherlands

Phone +31 30 2206 394

Fax +31 30 2202 570

Email weiss@knmi.nl

Keywords

Land-atmosphere coupling, potential predictability, EC-Earth, leaf area index

Abstract

Climate models often use a simplified and static representation of vegetation characteristics to determine fluxes of energy, momentum and water vapour between surface and lower atmosphere. In order to analyse the impact of short term variability in vegetation phenology, we use remotely-sensed leaf area index (LAI) and albedo products to examine the role of vegetation in the coupled land-atmosphere system. Perfect model experiments are carried out to determine the impact of realistic temporal variability of vegetation on potential predictability of evaporation and temperature, as well as model skill of EC-Earth simulations. The length of the simulation period is hereby limited by the availability of satellite products to 2000-2010. While a realistic representation of vegetation positively influences the simulation of evaporation and its potential predictability, a positive impact on 2m temperature is of smaller magnitude, regionally confined and more pronounced in climatically extreme years.

Introduction

In the light of seasonal-to-decadal climate predictions, a number of studies have recently focused on quantifying the fraction of low frequency variability, i.e. the potentially predictable climate component in relation to its sum with high frequency variability, i.e. the noise component. These analyses identify areas on the globe where climate variability is predictable on seasonal to decadal time scales. It is generally agreed that the state of a climate variable is a composite of an externally forced component (e.g. greenhouse gas (GHG) concentration, volcanic aerosols, land use change), a slowly evolving internal component (i.e. large scale ocean states, or behaviour of the coupled atmosphere-ocean system) and a rapidly fluctuating component (atmospheric noise) (Boer and Lambert 2008; George and Sutton 2006; Boer 2004).

Under the assumption that long-term fluctuations of sea surface temperatures (SSTs) are predictable, ensemble integrations can be used to quantify their subsequent influence on the atmosphere (Rowell 1998). In perfect model ensemble experiments, where the model is forced with realistic observed SST data, the atmospheric noise component is quantified by the ensemble spread resulting from different atmospheric initial conditions. The signal component is calculated from the ensemble mean variance over time. Potential predictability compares the signal variance to the total variance, i.e. the sum of signal and noise.

Previous studies have found higher values of SST-related potential predictability of surface air temperature predominantly over mid- to high latitude oceans (Boer and Lambert 2008; Boer 2004), and in the North Atlantic region (Pohlmann et al. 2004) with only weak signals over land in all of the studies. These results, in a way, stand in contrast to societal needs. Societal interest in climate predictability is greater for land areas, and also anthropogenic interference with the climate system originates from land areas. If extreme climatic events, for example droughts and floods, can be predicted well in advance, their consequences might be reduced or even avoided.

Inspired by these facts, the question we seek to answer in this study is whether slowly varying land surface properties exist that generate potentially predictable

variability in the atmosphere. We explore whether the land surface representation in an atmosphere-ocean general circulation model (AOGCM) can be improved in order to prolong the duration of the memory effect of past climate anomalies and their subsequent persistent influence on the atmosphere on longer (and thus potentially predictable) time scales. This question was initially raised by Venzke et al. (1999) and Rowell (1998). Subsequent studies on the role of soil-moisture and soil-moisture memory on land-atmosphere feedbacks have further underlined its potential and relevance. However these studies found a comparably lower impact of land variables on atmospheric states than for example the ocean exerts. Specific atmospheric and land surface state conditions are required for a strong land impact on the atmosphere, which is often regionally confined, (Dirmeyer 2005; van den Hurk et al. 2010; Koster et al. 2011; Gao et al. 2008; Dirmeyer 2009; Douville 2003; Guillevic et al. 2002; Koster et al. 2002; Koster et al. 2000; Reale and Dirmeyer 2002). Further extending these studies, here we seek to analyse the connection between soil-moisture and the atmosphere as it is reflected by plant physiology and short-term variability within.

Land surface and atmosphere are coupled through biophysical and biogeochemical processes (the latter are not covered in this study). In biophysical processes, atmosphere and land exchange energy, momentum and water fluxes (Arora and Boer 2006; Brovkin 2002). Anomalies in these fluxes induced by atmospheric variability should therefore be communicated back to the atmosphere (Dirmeyer and Zhao 2004) with some delay via modified evaporation, modified energy partitioning between latent heat and sensible heat fluxes, and modified upward radiation fluxes. A crucial link between land and atmosphere is vegetation, as it is both influenced by and reflects surface and subsurface states (e.g. soil moisture, runoff) and atmospheric states (e.g. temperature, vapour pressure deficit) (Dirmeyer and Zhao 2004; Douville 2003).

To test whether a perfect representation of vegetation is able to increase potential predictability over land, perfect model experiments are carried out as atmosphere-only simulations forced with observed SST fields. These are used to determine the increase in potential predictability calculated from coupled land-atmosphere general circulation model ensembles forced by observed, time-varying vegetation

distribution and phenology in comparison to a vegetation climatology. If an improved representation of land surface properties increases potential predictability, experiments with realistic temporal variability of vegetation should lead to significantly different climatic states and variability in comparison to vegetation climatology experiments. An increase of the signal component due to observed leaf area index (LAI) values and its quantification might further provide an estimate of the expected impact of coupled dynamic vegetation simulations on the atmosphere.

Potential predictability is defined here as the fraction of signal variance that is generated over the timescale of interest to the variance that is caused by short timescale instabilities, i.e. atmospheric noise (represented by e.g. using different atmospheric initial conditions in an ensemble experiment). The evolution of signal and noise variances can hence be followed separately. Potential predictability should be seen as an upper limit of the climate predictability of the model, reflecting the underlying assumptions of perfect model performance (Rowell 1998) and initialization. It is not stringently a measure for real predictability (evaluation against observations). Therefore, in addition to potential predictability we further compare modelled 2m temperature with reanalysis and observational data to verify whether an increase in potential predictability is concurrently associated with a decrease in model bias (increase in model skill).

Climate models usually exhibit a very high value of potential predictability up to approximately 2 weeks after initialization, which is lost afterwards due to the nonlinearity of the system (Lorenz 1982; Zwiers and Kharin 1998). Here, we are explicitly interested in potential predictability at seasonal time scales calculated from 10-year model runs.

The structure of the paper is as follows. Model, preparation of the input data and experimental design are described in section 2. The difference in potential predictability of land evaporation and land surface temperature between the different experiments are shown and discussed in section 3, as well as the quantification of model skill. Section 4 discusses and concludes the study.

Materials and Methods

EC-Earth and the land surface scheme HTESSEL

Calculations of potential predictability are based on EC-Earth version 2.2, a fully coupled AOGCM (Hazeleger et al. 2011; Hazeleger et al. 2010). In the configuration used in this study, ocean (NEMO2) and sea ice (LIM2) schemes are switched off and replaced by prescribed SST fields and sea-ice extent, based on re-analysis data (ERA-interim). The atmosphere module of EC-Earth strongly resembles the integrated forecast system (IFS) CY31 of the numerical weather prediction model of the European Center for Medium Range Weather Forecast (ECMWF), with some updates (the land surface and convection scheme) from a later cycle CY33. Model runs are carried out at a resolution of T159L62. For a more detailed model description, see Hazeleger et al. (2011).

The land surface scheme HTESSEL is based on the version described by van den Hurk et al. (2003; 2000) with a revised snow scheme (Dutra et al. 2010; Balsamo et al. 2009). For the calculation of surface fluxes, each grid cell is partitioned into different tiles of bare soil, high vegetation, low vegetation, intercepted water, shaded snow (under high vegetation) and exposed snow (on top of low vegetation or bare soil). Total fluxes are calculated as weighted average of individual surface energy balances per tile based on the resistance approach, where aerodynamic and surface resistances account for the transfer efficiency of heat and water vapour over a vertical temperature and humidity gradient.

Vegetation directly influences evaporation through transpiration and interception, and can tap lower layers of soil water depending on vegetation-specific rooting depth, in contrast to bare soil evaporation which evaporates water only from the top layer. In the default configuration of EC-Earth2.2, LAI fields (see following section) are based on ground surveys and model-internally extrapolated using spatial fields of vegetation cover and dominant vegetation types. Vegetation hereby remains fully developed throughout the year and shows no annual cycle. Surface albedo does vary over the season and is a composite of (background) land surface albedo based on monthly climatological Moderate Resolution Imaging Spectroradiometer (MODIS) averages, and dynamic snow albedo based on the

dynamical calculation of snow extent (Dutra et al. 2010). In the standard set-up, vegetation has no direct impact on land surface albedo.

Leaf area index

The state of vegetation reflects growing conditions such as atmospheric temperature, radiation inputs, and the level of soil moisture saturation. Its phenology usually exhibits a pronounced seasonal cycle. On vegetated surfaces, stomata in leaves are responsible for a great fraction of the water vapour (and energy) exchange between land and atmosphere (Buermann et al. 2002). Hence, LAI is often used as surrogate for the state and development stage of vegetation. Defined as the one sided leaf area per unit ground area, LAI determines important structural properties of plant canopies.

In this study the default EC-Earth2.2 configuration of using prescribed LAI values is replaced by using monthly values derived from remote sensing observations from MODIS on board of the TERRA satellite. The MOD15A2 collection 5 LAI product is a global data product composited over an 8-day period at 1km resolution, and available from the year 2000 onwards. It is derived from a three-dimensional radiative transfer model driven by an atmosphere corrected surface reflectance product (MOD09), a land cover product (MOD12) and ancillary information on surface characteristics. These data are distributed by the Land Processes Distributed Active Archive Center (LP DAAC), located at the U.S. Geological Survey (USGS) Earth Resources Observation and Science (EROS) Center (lpdaac.usgs.gov).

The preparation of an LAI climatology from MOD15A2 LAI collection 5 data is described by Boussetta et al. (2011) and Jarlan et al. (2008). The use of this LAI data set is operational at ECMWF from IFS Cycle 36 onwards. MOD15A2 data is re-projected and averaged to 1/12 degrees spatial resolution. The data is then spatially and temporally smoothed and monthly averages are calculated.

Monthly data for the individual years 2000-2010 contain gaps due to cloud cover restrictions. They are, after re-projection, gap-filled by searching for the closest

cell with the same land cover within a box of maximal 20°x20° geographical longitude and latitude. If no corresponding grid box is found, the climatological value for that grid-cell is used.

Both climatology and monthly data sets are finally interpolated to the native EC-Earth resolution (T159). Similar as in previous analyses of LAI variability (Buermann et al. 2002; Guillevic et al. 2002), we find high variability of measured LAI over the tropics throughout the year, and in the Northern and Southern hemisphere during the main growing periods April to August and October to February, respectively. Figure 1 shows the standard deviation of maximum LAI per growing season.

Surface albedo

Surface albedo determines the partitioning of incoming solar radiation into a reflected part and an absorbed part and plays a central role in the determination of the energy balance at the surface. In order to analyse the effect of LAI changes on the reflectance properties of the earth's surface, again, we use MODIS satellite data. The Filled Land Surface Albedo Map Product (MOD43B3) (Moody et al. 2008) provides five years (2000-2004) of spatially complete snow-free land surface albedo. The data was prepared using an ecosystem-dependant temporal interpolation technique (Moody et al. 2008). It is available on a 1 minute equal angle lat-lon grid in a temporal resolution of 16 days, as well as 5-year climatology. For testing the albedo effect with EC-Earth2.2, the broadband (0.3-5.0 μm) 8-day product is interpolated to monthly values. We then calculate monthly albedo anomalies, which are superimposed onto the default monthly EC-Earth albedo maps at T159 spatial resolution.

Experimental design

Four ensemble experiments are run from 2000-2010, with 10 members per ensemble that differ in their atmospheric initial conditions of January 1st, 2000, generated using singular vectors (Leutbecher 2007). The state of the ocean is prescribed based on the ERA-Interim SST and sea ice data (Dee et al. 2011).

Experiments 0 to 2 (see Table 1) differ only with respect to LAI. E0 is the control experiment with standard EC-Earth2.2 LAI values. In Experiment E1, monthly climatological LAI fields from MODIS are used. Experiment E2 uses time-varying ("perfect") monthly LAI fields, while in Experiment E3 this is complemented by also including ("perfect") monthly varying albedo fields. Due to the limited availability of albedo data, E3 only covers the 5-year period 2000-2004. Impacts on surface roughness length are not considered as part of this study. Its variation with LAI is considered to be small, in contrast to a stronger sensitivity for varying land cover, e.g. due to (de-)forestation.

Potential predictability

Potential predictability (PP) compares the signal variance σ_v^2 to the total variance σ^2, i.e. the sum of signal and noise, of a climate variable (eq. 2):

$$\sigma^2 = \sigma_v^2+\sigma_e^2 \qquad (1)$$

$$PP=\sigma_v^2/\sigma^2 \qquad (2)$$

The signal component is common to all forecasts initialized at the same point in time and can therefore be extracted from the variability of the ensemble mean over time (George and Sutton 2006). Hereby, we consider model simulations with a length of 10 years for experiments E0-E2, and 5 years for experiment E3, respectively (see **Table 1**). The difference between ensemble members, i.e. the ensemble spread, is associated with the noise component σ_e^2. As conclusively discussed in previous studies, a prime statistical tool is Analysis of Variance (ANOVA) to attribute different sources of variation (Rowell 1998; Boer 2004; Dirmeyer 2005).

The value of potential predictability being statistically significant different from zero is evaluated at the 95% level, based on an F-test as in Storch and Zwiers, (2002). For analysing the impact of vegetation on potential predictability, we use confidence intervals around PP to assess whether changes in PP are statistically significant, as described in Rowell (1998), again using F-statistics at the 95% confidence level.

Predictability / model skill

Model skill (predictability) is evaluated by comparing simulated temperature with two reference datasets: one observational (CRU TS 3.1) and one reanalysis (ERA-Interim) dataset.

The newest dataset of the University of East Anglia Climatic Research Unit, CRU TS 3.1 (Jones and Harris 2008), offers gridded time series of monthly climate parameters for the period 1901-2009. These are interpolated measurements from up to 4000 weather stations around the world, but station density significantly varies over time.

ERA-Interim (Dee et al. 2011) is a ECMWF global atmospheric reanalysis of the period 1979 to present and is based on cycle 31r2 of ECMWF's Integrated Forecast System (IFS), which was introduced operationally in September 2006.

Results

Potential predictability

Potential predictability of evaporation in experiment E2, which is significantly different from zero, is found over almost all land areas except in some (cold) desert areas (see Figure 2). We show values for the summer months of the respective hemispheres, i.e. months June to August for 0°N to 90°N, and months December to February for 0°S to 90°S, because the impact of LAI variability is most pronounced in its high season. Higher values of potential predictability (>0.45) are present in the tropics, South America, Australia, and in the forest areas of Russia, China, and India (blue areas in Figure 2). These high values of potential predictability are possibly to some extent caused by the prescribed ("perfect") SST data. Nonetheless, we find "perfect" LAI exhibiting an almost exclusively positive impact on seasonal potential predictability of summer evaporation, leading to higher absolute values throughout the globe. Figure 3 shows the gain in PP of evaporation that we achieve by replacing the climatological LAI values in E1 with the time varying data in E2, confirming that the interannual variability in LAI does emerge as a detectable variability in evaporation. These areas coincide with areas of strong interannual variability of LAI in the summer (compare Figure 1).

Figures 2 and 3 further show a strong spatial variability of PP, related to stronger spatial gradients due to un-smoothed LAI values in experiment E2 than in E0 or E1. Hardly any change in PP of evaporation is found over barely vegetated areas, such as the Sahara, Mongolia and very high Northern latitudes.

Higher values of potential predictability of 2m temperature (T2m) are present only in the tropics, over a belt stretching from app. 30°N – 30°S (not shown). Although we find a positive impact of time-varying LAI values (moving from E1 to E2) especially in the Northern hemisphere during summer (Figure 4), e.g. over forested areas of North America, India, and parts of Europe and Russia, absolute potential predictability does not exceed 0.2 here. Potential predictability of T2m decreases slightly over the Amazon and reduces PP there. The PP gain for

temperature is in general smaller than for evaporation, since changes in LAI only indirectly influence temperature via evaporation, and competes with the impact of other processes, such as atmospheric circulation on surface temperatures.

The additional increase in potential predictability of summer T2m, due to further considering time-varying albedo (Exp E3 – E2), is shown in Figure 4. Note that this experiment covers the 5-year period 2000 – 2004. The effect of including observed albedo exceeds the increase in PP of temperature obtained with time varying LAI (Exp E2 – E1) after five years (2000-2004) in many areas (not shown). Increase of PP for E3-E2 is more localized, and in general, the change in PP is in more areas not statistically significant at the 95% level due to the shorter time period considered. Areas are present, where PP decreases upon introduction of observed albedo, presumably due to opposing impacts of LAI (via evaporation) and albedo (via radiation) on temperature.

Total variance of T2m is highest in the Northern hemisphere and decreases southwards. This variance is amplified as variability is added to the factors contributing to this variance, such as time varying LAI values (Koster et al. 2000). Figure 6 shows this total variance amplification that results from switching from climatological (E1) to time varying LAI values (E2) for surface temperature. Total variance amplifies mainly in the Northern hemisphere and partly in the tropics. These areas coincide with areas with a negative correlation between soil-moisture and evapotranspiration in spring and summer (Dirmeyer 2009, their Figure 3). In these areas, Dirmeyer et al. (2009) do not expect a strong hydrological coupling between land and atmosphere, since evaporation is not controlled by soil moisture but instead evaporation affects soil moisture by depletion. However, Figure 3 shows that in these areas a positive impact of time varying LAI values on temperature variability is found. Changes in LAI affect evapotranspiration more strongly in non-water limited, i.e. radiation limited climate regimes, where a change in vegetation properties can translate into evapotranspiration- and subsequent temperature changes. In areas where evaporation is soil moisture limited, changes in LAI are not as effective.

Comparing Figure 6 and Figure 1, T2m variance amplification coincides with areas of high LAI amplitude variability. In order to examine the relationship between the variability in seasonal LAI amplitude, season length, and T2m signal further, we apply the TIMESAT program package, developed by Jönsson and Eklundh (2004) to the LAI satellite data. This software enables the investigation of the seasonality of satellite time series data by fitting asymmetric Gaussian functions based on least squares fits through the LAI series. Different land cover classes can be distinguished. From these functions, season length and LAI amplitude per growing season can be determined (Jönsson and Eklundh 2004).

Strongest increases in signal variability σ_v^2 are found in the Northern hemisphere, being caused by season length variability of approximately 1 month and LAI amplitude variability of about 0 to 0.4 m^2/m^2 (Figure 7). Both desert and tropical rainforest are vegetation types where the variability of the season length is high, while the amplitude variability is very low, for the desert at low absolute amplitude and for the tropics at high absolute amplitude. Adding LAI variability in tropical forests, i.e. very densely vegetated areas with high LAI increases evaporation variability, but this does not affect temperature variability. Therefore, we find increasing PP values for evaporation but not in all areas also for temperature. If noise variability decreases simultaneously with signal variability, increasing values of PP can still be found. However, fitting functions to monthly LAI time series is more difficult for vegetation types with less pronounced seasonal cycles that are additionally not synchronized with the calendar year, and where only small changes in absolute LAI values between seasons occur.

Model skill

For an evaluation of model skill two temperature data sets are used over the period 2000-2009: ERA-Interim and CRU TS 3.1. These data sets are shown to disagree considerably in certain areas (see Figure 8), as also found problematic in impact studies of Poulter et al. (2007) and Maignan (2011). Therefore, we evaluate model skill effects only in areas where the two data sets are consistent within an arbitrarily chosen range of ±1K.

Table 2 summarizes the gain in global model skill during the period 2000-2009 for the Northern hemisphere seasons winter (DJF), spring (MAM), summer (JJA), and autumn (SON), as well as for the annual average. Compared to CRU TS 3.1, we find a gradual reduction in model bias in all seasons for the experiments E0 to E2. Time varying LAI values appears to reduce the general cold bias of EC-Earth2.2, with a small overshoot in summer, where the model is too warm especially in North America and central Europe (not shown). The additional consideration of remotely-sensed albedo values (E3) reduces this warming effect, which leads to a better agreement of summer temperature values but cooler values in the other seasons.

Figure 9 and 10 show bias-corrected Root Mean square Error (rmse) and anomaly correlation for different hemispheres and 3 regions, being Europe (0°E-80°E, 70°N-40°N), US (130°W-60°W, 50°N – 20°N) and the Amazon (80°W-40°W, 10°N- 30°S). Europe shows the highest reduction in rmse. In the Southern hemisphere and the US, a small increase in rmse is found. All areas show an improved anomaly correlation with the observations. However, it is noted that in the Amazon a large number of gridcells was excluded from the comparison due to the disagreement between the ERA-Interim and CRU TS 3.1 datasets.

Overall, remotely sensed LAI is very heterogeneous. Spatial variability between gridcells is high and extreme values occur over small, locally confined areas, especially when analysed at the spatial resolution of EC-Earth. The positive impact of a more realistic LAI on model performance seems to become more

apparent in extreme years where actual LAI has the highest deviation from the climatologically value. Anomaly correlation of modelled and observed T2m improves if cells and years of extreme values of LAI amplitude or season length are selected, but this positive effect is levelled out if broader regions are analysed. We refrain from giving any further numerical or visual evidence because the extreme patchiness would lead to the invention of a number of filter rules. Nonetheless, the results hint towards slightly improved local agreement of simulated and observed meteorological variables in comparison to the regional, long-term averages.

Discussion

In general, “perfect” LAI values increase PP of evaporation. The impact on 2m temperature is less pronounced, and in certain areas PP it is reduced. These, however, are areas where absolute potential predictability is already high due to relatively low noise levels (for example the Amazon), or where vegetation is almost not present (as in deserts). The slightly negative impact on PP is compensated by a positive impact on 2m temperature skill in these areas and a bias reduction in general.

The systematic difference between mean surface temperature in the two datasets ERA-Interim and CRU TS 3.1 makes an overall assessment of the gain in skill difficult. While the quality of the reanalysis data strongly depends on model performance, measured data are not necessarily representative for the area of a grid cell due to possible local microclimatological and topographic effects (Simmons et al. 2004). CRU TS 3.1, for example, suffers from an extremely reduced station number from year 2000 onwards in comparison to the previous century.

Overall, an impact of LAI on both evaporation and temperature is noticeable. The difference between experiments E1 and E2 translate into a sensitivity of mean growing season evaporation of 0.24 mm/d per unit leaf area for NH and TR, and 0.32 mm/d for SH. The temperature sensitivity is on average -0.65K per unit leaf area for NH, and -0.47K for TR and SH. Effects of LAI on precipitation generally have a small or positive sign: 0.17 mm/d per unit leaf area for NH, 0.19 mm/d for SH, and ~0 for TR.

General drawbacks of remotely sensed data apply. Specifically, for MODIS LAI this includes an overestimation of the monthly variability in densely vegetated areas, such as the tropics, due to low surface reflectance sensitivity at high LAI values (saturation) and temporarily high cloud cover, as well as overestimation of seasonal LAI in boreal forests due to limitations of the radiative transfer algorithm (Yang et al. 2006). However, previous studies have confirmed acceptable

agreement between measured field values and remotely sensed datasets, including the seasonal variation of LAI in the tropics (Myneni et al. 2007; Garrigues et al. 2008)

Although the time varying LAI in E2 possibly reflects vegetation responses to historical atmospheric conditions and has the ability to provide some feedback to the atmosphere, the time-scale on which this effect is seen, remains limited. An impact that emerges from the general atmospheric noise is mainly visible during extreme conditions, where both the signal variance is increased (positive impact on PP) and the model skill is slightly improved. For states closer to climatology, the effect is overwhelmed by the atmospheric noise. Generally, the memory of the land component is with a typical duration of months to seasons comparably short (Dirmeyer 2009). Yet, longer modes with periods of 3 to 4 years have been detected in vegetation by Los et al. (2001; as cited in Guillevic et al. 2002) that apparently correspond to ENSO and NAO indices. The length of the simulations carried out here is too short to detect these longer cycles with adequate robustness. The limited simulation length possibly also leads to an underestimation of the signal variance σ_v^2 and of the LAI variability. Long-lasting LAI anomalies that stretch over a decade do exist, such as extended droughts in China (Xiao et al. 2009), which were not detectable here due to the length of the available satellite data.

Coupled simulations, where LAI is calculated interactively within the atmospheric model, might increase the interannual variability of evaporation and, to a smaller extent, of surface temperature. A feedback loop between vegetation and the atmosphere, where atmospheric anomalies feed back to anomalies in vegetation and resulting evaporation, was not represented in the present experimental design, but could further amplify or dampen these responses.

Summary and conclusions

In this study, perfect model experiments were carried out to examine the role of vegetation phenology for potential predictability and model skill over land areas. Replacing the LAI climatology by realistic time varying LAI values increases potential predictability of summer evaporation. Significant gains in potential predictability are found in tropical areas and forested areas of Russia, India and Australia. The impact on the potential predictability of 2m summer temperature is less pronounced and not positive in all areas. Potential predictability of 2m temperature is not increased to significant values outside the tropics, but model skill improves on a global average. While the impact on evaporation is clearly positive, the effect on 2m temperature is smaller and therefore more likely to be drowned by atmospheric noise.

A drawback of the current model set-up is that processes are not fully coupled. The atmospheric model is exposed to a realistic representation of vegetation, which influences soil moisture levels and the state of the atmosphere via evaporation, but a subsequent impact on vegetation in the next model-step is not included in the model formulation, but imposed by external data sets. To include this feedback, further model experiments with a coupled dynamic vegetation model are required. This would a) close the missing link in land-atmosphere coupling and b) enable the extension of the experiment to longer time-scales. Availability of LAI satellite data restricted experiments of the present study to the decade 2000-2010. Longer runs (e.g. century or more) could further increase the sampled signal variance due to inclusion of a larger sample of climatic states, and signal and noise might be separated more robustly.

The present results indicate that this vegetation – climate interaction indeed will lead to different variability in surface evaporation and near surface temperatures, and will thus exhibit a discernible signal in the simulations that should be verified using observations. Since the state of vegetation influences only a small aspect of the process chain of land-atmosphere coupling, it cannot compensate for under-represented processes. However, in combination with further improved and fully-coupled land-surface processes (for example landcover changes, or interactive carbon cycle), the inclusion of the actual state of vegetation seems promising to

further improve potential predictability and skill of climate models, but will also always be an additional source of noise due to its spatial heterogeneity.

Acknowledgements

This work was funded by the European Commission's 7th Framework Programme, under Grant Agreement number 226520, COMBINE project.

Figures & Tables

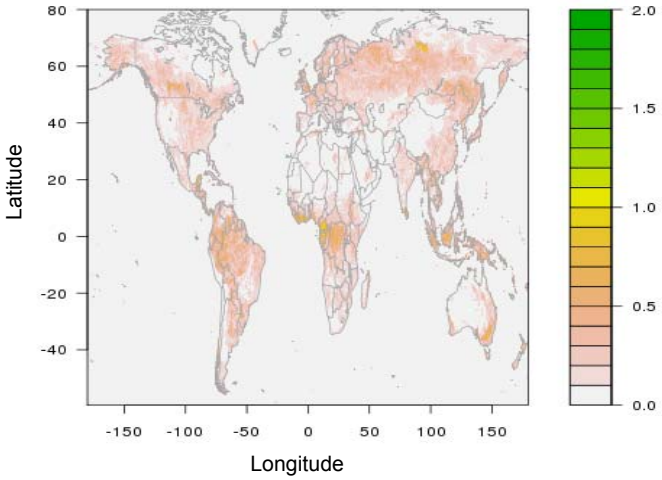

Figure 1: Standard deviation in maximum LAI value ("LAI amplitude") per growing season for the period 2000-2010

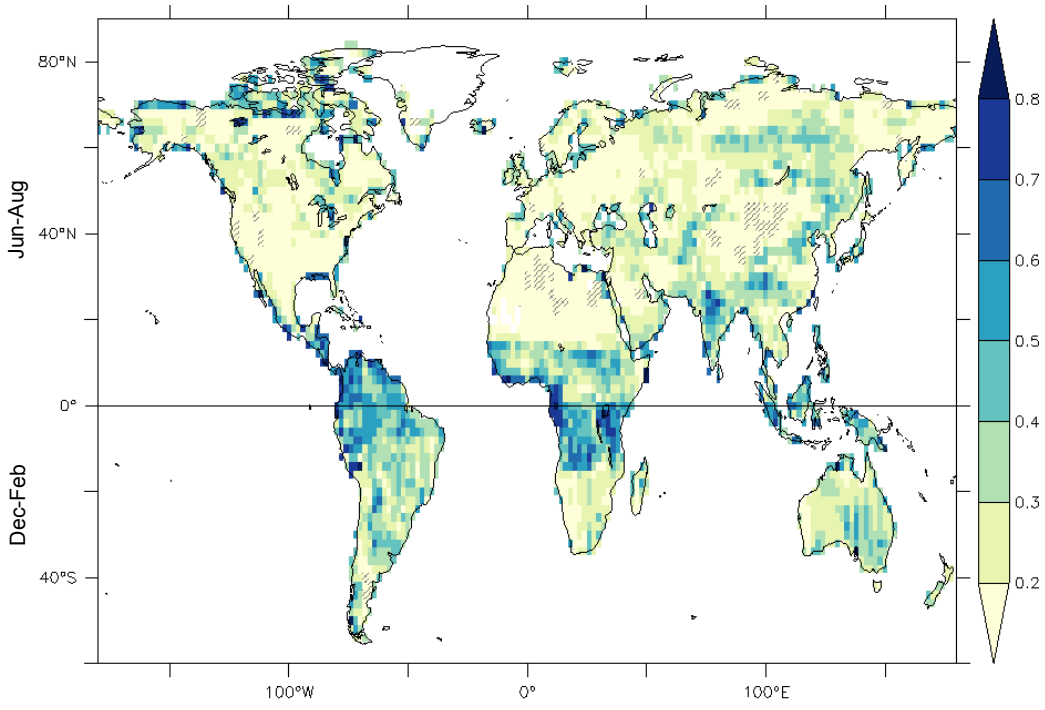

Figure 2. Seasonal potential predictability of summer land evaporation using observed time varying LAI values (Exp E2 covering 2000-2010), calculated using Eq 2. Note that summer is defined as months July to August for 0°N to 90°N and as months December to February for 0°S to 90°S. Hatched areas are not statistically significant at 95% level.

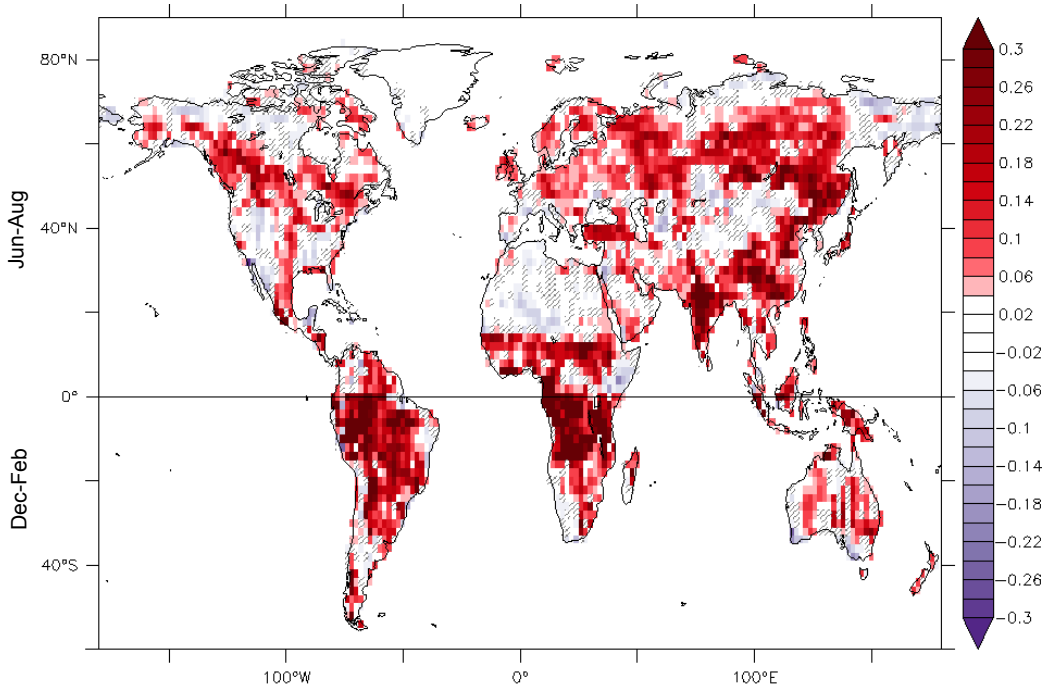

Figure 3. Gain in potential predictability of evaporation during summer due to switching from climatological to time varying LAI values (PP of Exp E2 minus E1, 2000-2010). Summer is defined as in Fig 1. Hatched areas are not statistically significant at 95% level.

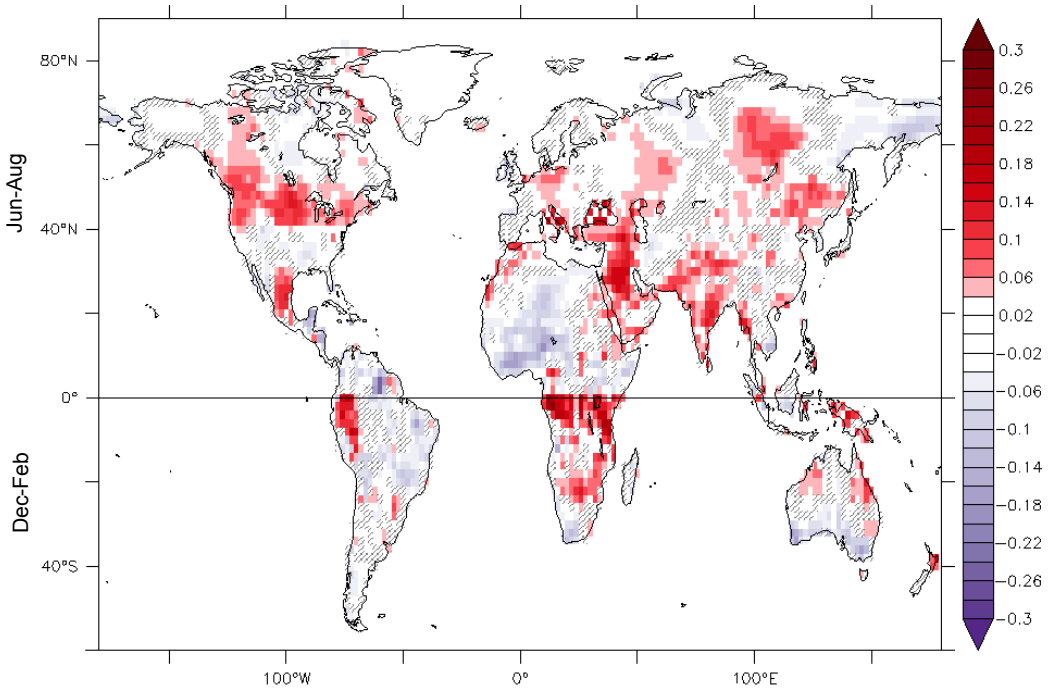

Figure 4. As Figure 3 for 2m temperature in summer.

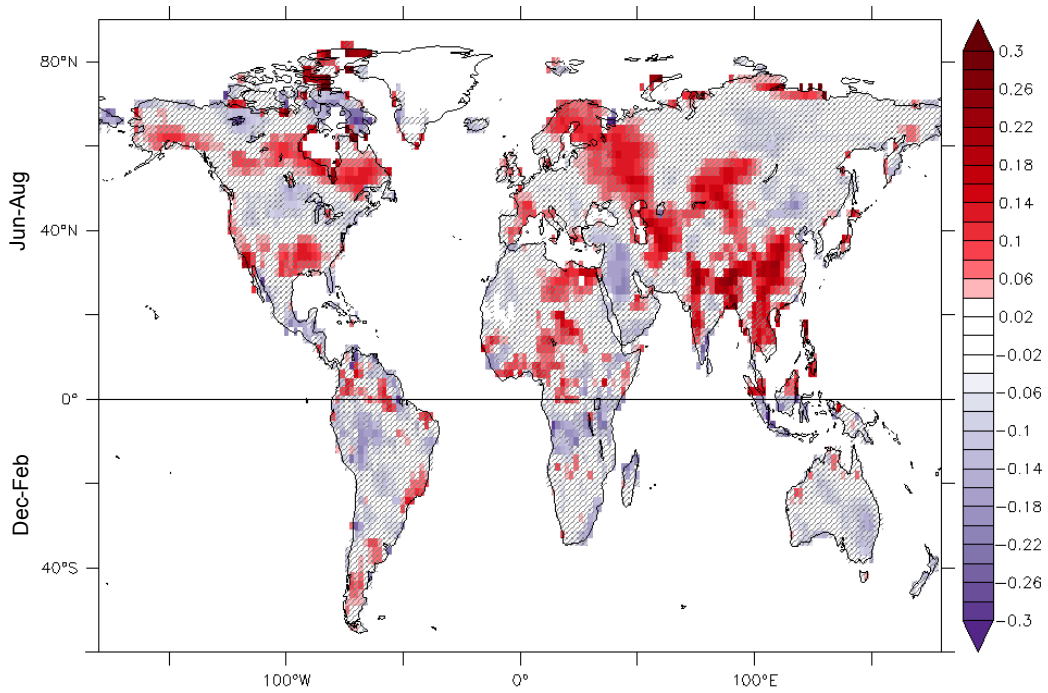

Figure 5. Gain in PP of 2m temperature in summer due to additionally including albedo changes (PP Exp E3 – E2; 2000-2004). Summer is defined as in Fig 1.

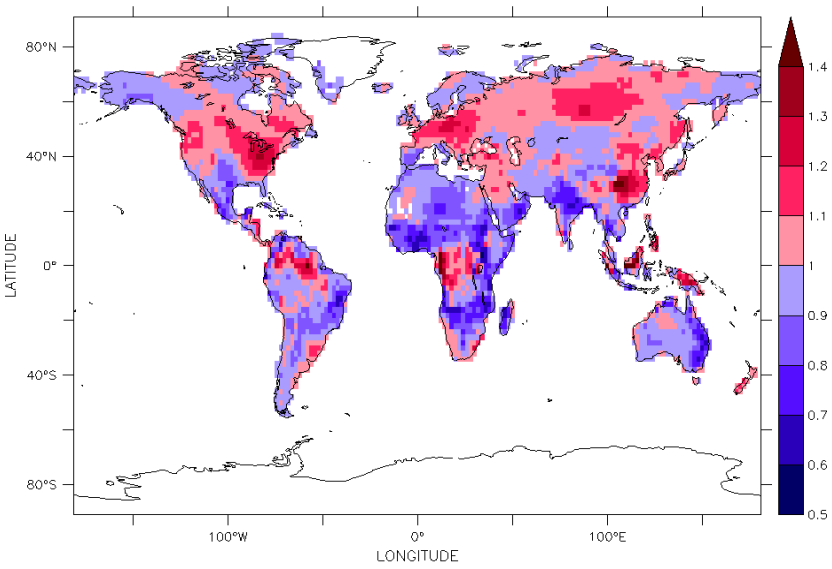

Figure 6. Total T2m variance amplification, defined as σ^2 (E2) / σ^2 (E1)

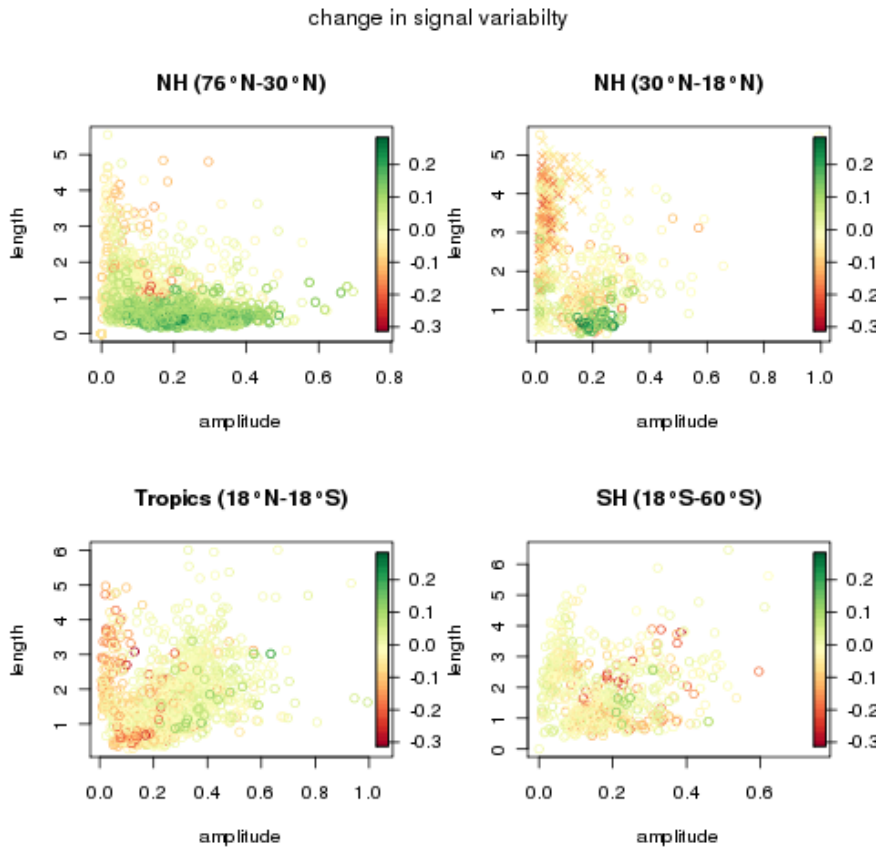

575

576

577 **Figure 7. Difference in T2m signal variability σ_v^2 between exp E0 and E1 (colour coded) as**
578 **function of changes in LAI season length and amplitude. Each symbol denotes a grid point,**
579 **and different latitude bands are shown in different panels (see panel titles). The upper right**
580 **panel further differentiates the Sahara from the rest of the considered land cells as crosses.**

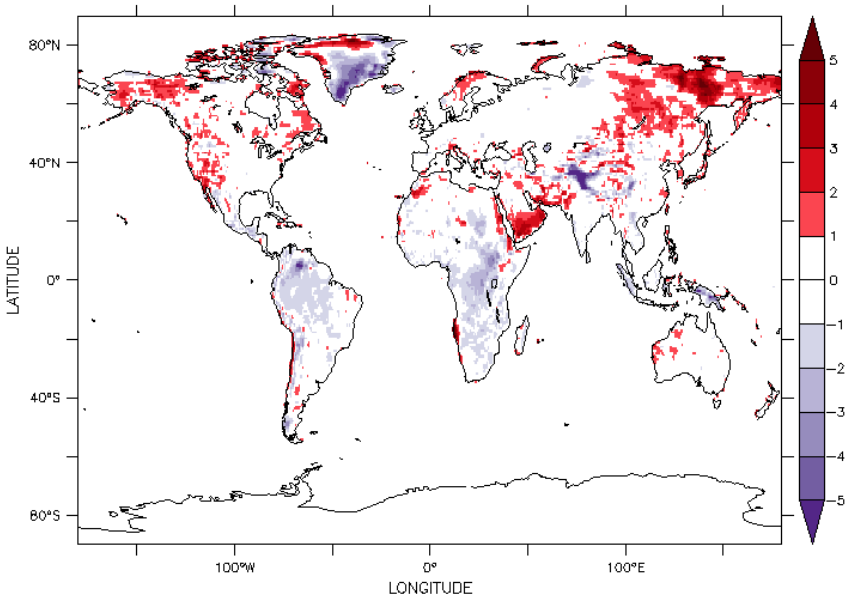

Figure 8: Annual mean temperature difference between ERA-Interim reanalysis and CRU TS 3.1 averaged over 2000-2009.

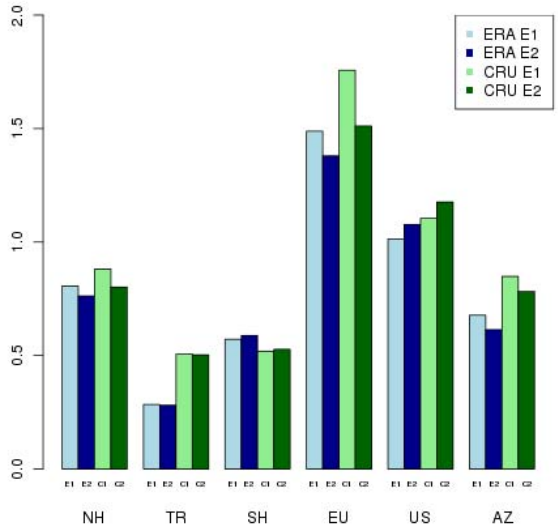

Figure 9. Bias -reduced root mean square error of temperature averaged over 2000-2009 for the Northern hemisphere (NH), Tropics (TR) and Southern hemisphere (SH), and three regions Europe (EU), United States and Canada (US) and the Amazon (AZ) relative to two datasets: ERA-Interim (E) in blue and CRU TS 3.1 (C) in green for experiments E1 (1) in light colour and E2 (2) in dark colour.

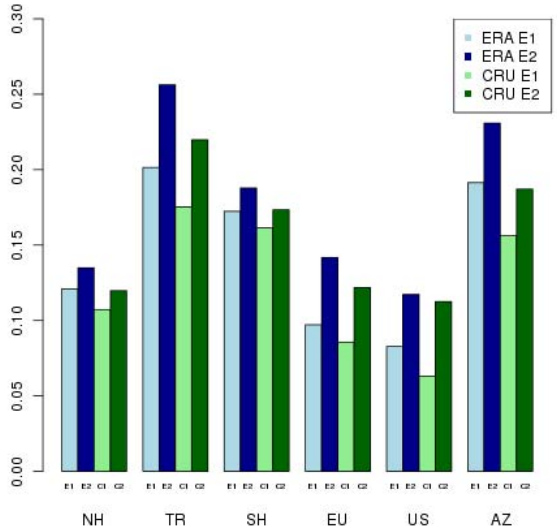

Figure 10. As figure 9, for the anomaly correlation of modelled vs. observed annual mean temperature averaged over 2000-2009.

600

601 **Table 1. Description of experiments**

Experiment identifier	No. of ensemble members	Time period of simulations	Experiment description
E0	10	2000-2010	constant LAI (fully developed through-out the year)
E1	10	2000-2010	climatological LAI (12 monthly values)
E2	10	2000-2010	monthly LAI from satellite data
E3	10	2000-2004	monthly LAI and albedo from satellite data

602

603 **Table 2. Global average difference between modelled (EC-Earth2) and observed (CRU TS**
604 **3.1) 2m temperature 2000-2009 of experiments E0 to E2 (model bias).**

605

experiment	annual avg	DJF	MAM	JJA	SON
E0	-1.014	-0.644	-1.236	-1.021	-1.040
E1	-0.749	-0.687	-0.880	-0.504	-0.788
E2	-0.232	-0.428	-0.350	0.321	-0.322

606

607

608 **Table 3. As Table 2, for experiments E2 and E3 in the period 2000-2004.**

609

experiment	annual avg	DJF	MAM	JJA	SON
E2	-0.202	-0.540	-0.333	0.317	-0.243
E3	-0.451	-0.923	-0.537	0.253	-0.572

610

References

Arora VK, Boer GJ (2006) The Temporal Variability of Soil Moisture and Surface Hydrological Quantities in a Climate Model. Journal of Climate 19 (22):5875-5888. doi:10.1175/jcli3926.1

Balsamo G, Beljaars A, Scipal K, Viterbo P, van den Hurk B, Hirschi M, Betts AK (2009) A Revised Hydrology for the ECMWF Model: Verification from Field Site to Terrestrial Water Storage and Impact in the Integrated Forecast System. Journal of Hydrometeorology 10 (3):623-643. doi:doi:10.1175/2008JHM1068.1

Boer GJ (2004) Long time-scale potential predictability in an ensemble of coupled climate models. Climate Dynamics 23 (1):29-44. doi:10.1007/s00382-004-0419-8

Boer GJ, Lambert SJ (2008) Multi-model decadal potential predictability of precipitation and temperature. Geophys Res Lett 35 (5):L05706. doi:10.1029/2008gl033234

Boussetta S, Balsamo G, Beljaars A, Kral T, Jarlan L (2011) Impact of a satellite-derived Leaf Area Index monthly climatology in a global Numerical Weather Prediction model. Int J Remote Sensing (accepted)

Brovkin V (2002) Climate-vegetation interaction. J Phys IV France 12 (10):57-72

Buermann W, Wang Y, Dong J, Zhou L, Zeng X, Dickinson RE, Potter CS, Myneni RB (2002) Analysis of a multiyear global vegetation leaf area index data set. J Geophys Res 107 (D22):4646. doi:10.1029/2001jd000975

Dee DP, Uppala SM, Simmons AJ, Berrisford P, Poli P, Kobayashi S, Andrae U, Balmaseda MA, Balsamo G, Bauer P, Bechtold P, Beljaars ACM, van de Berg L, Bidlot J, Bormann N, Delsol C, Dragani R, Fuentes M, Geer AJ, Haimberger L, Healy SB, Hersbach H, Hólm EV, Isaksen L, Kållberg P, Köhler M, Matricardi M, McNally AP, Monge-Sanz BM, Morcrette JJ, Park BK, Peubey C, de Rosnay P, Tavolato C, Thépaut JN, Vitart F (2011) The ERA-Interim reanalysis: configuration and performance of the data assimilation system. QJR Meteorol Soc 137:553-597. doi:10.1002/qj.828

van den Hurk B, Doblas-Reyes F, Balsamo G, Koster R, Seneviratne S, Camargo H (2010) Soil moisture effects on seasonal temperature and precipitation forecast scores in Europe. Climate Dynamics:1-14. doi:10.1007/s00382-010-0956-2

van den Hurk BJJM, P.Viterbo, Beljaars ACM, Betts AK (2000) Offline validation of the ERA40 surface scheme. ECMWF Tech Memo ECMWF,

van den Hurk BJJM, Viterbo P, Los SO (2003) Impact of leaf area index seasonality on the annual land surface evaporation in a global circulation model. J Geophys Res 108 (D6):4191. doi:10.1029/2002jd002846

Dirmeyer PA (2005) The Land Surface Contribution to the Potential Predictability of Boreal Summer Season Climate. Journal of Hydrometeorology 6 (5):618-632. doi:10.1175/jhm444.1

Dirmeyer PA, C. Adam Schlosser, Kaye L. Brubaker (2009) Precipitation, recycling, and land memory: an integrated analysis. J Hydrometeor 10:278-288

Dirmeyer PA, Zhao M (2004) Flux Replacement as a Method to Diagnose Coupled Landâ€“Atmosphere Model Feedback. Journal of Hydrometeorology 5 (6):1034-1048. doi:10.1175/jhm-384.1

Douville H (2003) Assessing the Influence of Soil Moisture on Seasonal Climate Variability with AGCMs. Journal of Hydrometeorology 4 (6):1044-1066. doi:10.1175/1525-7541(2003)004<1044:atiosm>2.0.co;2

Dutra E, Balsamo G, Viterbo P, Miranda PMA, Beljaars A, Schär C, Elder K (2010) An Improved Snow Scheme for the ECMWF Land Surface Model: Description and Offline Validation. Journal of Hydrometeorology 11 (4):899-916. doi:doi:10.1175/2010JHM1249.1

Gao X, Dirmeyer PA, Guo Z, Zhao M (2008) Sensitivity of Land Surface Simulations to the Treatment of Vegetation Properties and the Implications for Seasonal Climate Prediction. Journal of Hydrometeorology 9 (3):348-366. doi:10.1175/2007jhm931.1

Garrigues S, Lacaze R, Baret F, Morisette JT, Weiss M, Nickeson JE, Fernandes R, Plummer S, Shabanov NV, Myneni RB, Knyazikhin Y, Yang W (2008) Validation and intercomparison of global Leaf Area Index products derived from remote sensing data. J Geophys Res 113 (G2):G02028. doi:10.1029/2007jg000635

George SE, Sutton RT (2006) Predictability and skill of boreal winter forecasts made with the ECMWF Seasonal Forecasting System II. QJR Meteorol Soc 132:2031-2053. doi:10.1256/qj.04.180

Guillevic P, Koster RD, Suarez MJ, Bounoua L, Collatz GJ, Los SO, Mahanama SPP (2002) Influence of the interannual variability of vegetation on the surface energy balance-a global sensitivity study. J Hydrometeor 3:617-629. doi:10.1175/1525-7541(2002)003<0617:IOTIVO>2.0.CO;2

Hazeleger W, Severijns C, Semmler T, Ştefănescu S, Yang S, Wang X, Wyser K, Dutra E, Baldasano JM, Bintanja R, Bougeault P, Caballero R, Ekman AML, Christensen JH, van den Hurk B, Jimenez P, Jones C, Kållberg P, Koenigk T, McGrath R, Miranda P, Van Noije T, Palmer T, Parodi JA, Schmith T, Selten F, Storelvmo T, Sterl A, Tapamo H, Vancoppenolle M, Viterbo P, Willén U (2010) EC-Earth: A Seamless Earth-System Prediction Approach in Action. Bulletin of the American Meteorological Society 91 (10):1357-1363. doi:10.1175/2010bams2877.1

Hazeleger W, Wang X, Severijns C, Ştefănescu S, Bintanja R, Sterl A, Wyser K, Semmler T, Yang S, van den Hurk B, van Noije T, van der Linden E, van der Wiel K (2011) EC-Earth V2: description and validation of a new seamless Earth system prediction model. Submitted to Climate Dynamics

Jarlan L, Balsamo G, Lafont S, Beljaars A, Calvet JC, Mougin E (2008) Analysis of leaf area index in the ECMWF land surface model and impact on latent heat and carbon fluxes: Application to West Africa. J Geophys Res 113 (D24):D24117. doi:10.1029/2007jd009370

Jones P, Harris I (2008) CRU Time Series (TS) high resolution gridded datasets. CRU University of East Anglia Climate Research Unit,

NCAS British Atmospheric Data Centre. http://badc.nerc.ac.uk/view/badc.nerc.ac.uk__ATOM__dataent_1256223773328276.

Jönsson P, Eklundh L (2004) TIMESAT - a program for analysing time-series of satellite sensor data. Computers and Geosciences 30:833-845

Koster RD, Dirmeyer PA, Hahmann AN, Ijpelaar R, Tyahla L, Cox P, Suarez MJ (2002) Comparing the Degree of Land-Atmosphere Interaction in Four Atmospheric General Circulation Models. Journal of Hydrometeorology 3 (3):363-375. doi:10.1175/1525-7541(2002)003<0363:ctdola>2.0.co;2

Koster RD, Mahanama SPP, Yamada TJ, Balsamo G, Berg AA, Boisserie M, Dirmeyer PA, Doblas-Reyes FJ, Drewitt G, Gordon CT, Guo Z, Jeong JH, Lee WS, Li Z, Luo L, Malyshev S, Merryfield WJ, Seneviratne SI, Stanelle T, van den Hurk BJJM, Vitart F, Wood EF (2011) The Second Phase of the Global Land-Atmosphere Coupling Experiment: Soil Moisture Contributions to Subseasonal Forecast Skill. Journal of Hydrometeorology 12 (5):805-822. doi:10.1175/2011jhm1365.1

Koster RD, Suarez MJ, Heiser M (2000) Variance and Predictability of Precipitation at Seasonal-to-Interannual Timescales. Journal of Hydrometeorology 1 (1):26-46. doi:10.1175/1525-7541(2000)001<0026:vapopa>2.0.co;2

Leutbecher M (2007) On the representation of initial uncertainties with multiple sets of singular vectors optimized for different criteria. 133:2045-2056. doi:10.1002/qj.174

Lorenz EN (1982) Atmospheric predictability experiments with a large numerical model. Tellus 34 (6):505-513. doi:10.1111/j.2153-3490.1982.tb01839.x

Los SO, Collatz GJ, Bounoua L, Sellers PJ, Tucker CJ (2001) Global Interannual Variations in Sea Surface Temperature and Land Surface Vegetation, Air Temperature, and Precipitation. Journal of Climate 14 (7):1535-1549. doi:10.1175/1520-0442(2001)014<1535:giviss>2.0.co;2

Maignan F, Bréon F-M, Chevallier F, Viovy N, Ciais P, Garrec C, Trules J, Mancip M (2011) Evaluation of a Dynamic Global Vegetation Model using time series of satellite vegetation indices. Geosci Model Dev Discuss 4:907-941. doi:10.5194/gmdd-4-907-2011

Moody EG, King MD, Schaaf CB, Platnick S (2008) MODIS-Derived Spatially Complete Surface Albedo Products: Spatial and Temporal Pixel Distribution and Zonal Averages. Journal of Applied Meteorology and Climatology 47 (11):2879-2894. doi:10.1175/2008jamc1795.1

Myneni RB, Yang W, Nemani RR, Huete AR, Dickinson RE, Knyazikhin Y, Didan K, Fu R, Negrón Juárez RI, Saatchi SS, Hashimoto H, Ichii K, Shabanov NV, Tan B, Ratana P, Privette JL, Morisette JT, Vermote EF, Roy DP, Wolfe RE, Friedl MA, Running SW, Votava P, El-Saleous N, Devadiga S, Su Y, Salomonson VV (2007) Large seasonal swings in leaf area of Amazon rainforests. Proceedings of the National Academy of Sciences 104 (12):4820-4823. doi:10.1073/pnas.0611338104

729 Pohlmann H, Botzet M, Latif M, Roesch A, Wild M, Tschuck P (2004) Estimating the Decadal
730 Predictability of a Coupled AOGCM. Journal of Climate 17 (22):4463-4472.
731 doi:doi:10.1175/3209.1
732 Poulter B, Frank DC, Hodson EL, Zimmermann NE (2007) Impacts of land cover and climate data
733 selection on understanding terrestrial carbon dynamics and the CO2 airborne fraction.
734 Biogeosciences 8 (8). doi:10.5194/bg-8-2027-2011
735 Reale O, Dirmeyer P (2002) Modeling the Effect of Land Surface Evaporation Variability on
736 Precipitation Variability. Part I: General Response. Journal of Hydrometeorology 3
737 (4):433-450. doi:10.1175/1525-7541(2002)003<0433:mteols>2.0.co;2
738 Rowell DP (1998) Assessing Potential Seasonal Predictability with an Ensemble of Multidecadal
739 GCM Simulations. Journal of Climate 11 (2):109-120. doi:doi:10.1175/1520-
740 0442(1998)011<0109:APSPWA>2.0.CO;2
741 Simmons AJ, Jones PD, da Costa Bechtold V, Beljaars ACM, Kållberg PW, Saarinen S, Uppala
742 SM, Viterbo P, Wedi N (2004) Comparison of trends and low-frequency variability in
743 CRU, ERA-40, and NCEP/NCAR analyses of surface air temperature. J Geophys Res 109
744 (D24):D24115. doi:10.1029/2004jd005306
745 Storch Hv, Zwiers FW (2002) Statistical Analysis in Climate Research. Cambridge University
746 Press,
747 Venzke S, Allen MR, Sutton RT, Rowell DP (1999) The Atmospheric Response over the North
748 Atlantic to Decadal Changes in Sea Surface Temperature. Journal of Climate 12 (8):2562-
749 2584. doi:10.1175/1520-0442(1999)012<2562:tarotn>2.0.co;2
750 Xiao J, Zhuang Q, Liang E, Shao X, McGuire AD, Moody A, Kicklighter DW, Melillo JM (2009)
751 Twentieth-century droughts and their impacts on terrestrial carbon cycling in china. Earth
752 Interact 13:1-31. doi:10.1175/2009EI275.1
753 Yang W, Shabanov NV, Huang D, Wang W, Dickinson RE, Nemani RR, Knyazikhin Y, Myneni
754 RB (2006) Analysis of leaf area index products from combination of MODIS Terra and
755 Aqua data. Remote Sensing of Environment 104 (3):297-312
756 Zwiers FW, Kharin VV (1998) Intercomparison of interannual variability and potential
757 predictability: an AMIP diagnostic subproject. Climate Dynamics 14 (7):517-528.
758 doi:10.1007/s003820050238
759
760